Age, growth, and sexual dimorphism of the Southern Hemisphere long-finned pilot whale (*Globicephala melas edwardii*)

Emma L. Betty,[1],*,[ORCID] Karen A. Stockin,[1] Bethany Hinton,[1] Barbara A. Bollard,[2] Adam N.H. Smith,[3] Mark B. Orams,[4] and Sinéad Murphy[5,6]

[1]*Cetacean Ecology Research Group, School of Natural Sciences, College of Sciences, Massey University, Auckland, New Zealand*
[2]*School of Engineering, Mathematical and Computational Sciences, Faculty of Design and Creative Technologies, Auckland University of Technology, Auckland, New Zealand*
[3]*School of Computational Sciences, College of Sciences, Massey University, Auckland, New Zealand*
[4]*Faculty of Health and Environmental Sciences, Auckland University of Technology, Auckland, New Zealand*
[5]*Marine and Freshwater Research Centre, Department of Natural Sciences, School of Science and Computing, Galway-Mayo Institute of Technology, Galway, Ireland*
[6]*Institute of Zoology, Zoological Society of London, London, United Kingdom*

*To whom correspondence should be addressed: e.l.betty@massey.ac.nz

Knowledge of population biological parameters can contribute to assessing the resilience of a population in the face of increasing anthropogenic pressures. Southern Hemisphere long-finned pilot whales (*Globicephala melas edwardii*) are susceptible to high rates of live stranding-related mortality. However, the biological parameters of this population largely are unknown. In this study, age, growth, allometry, and sexual dimorphism are described using teeth and external body measurements obtained from 515 male, 776 female, and 229 individuals of unknown sex, stranded on the New Zealand coastline between 1948 and 2017. Maximum ages of 31 and 38 years were estimated for males (*n* = 163) and females (*n* = 239), respectively. Females ranged in length from 160 to 500 cm (modal size class 400–449 cm) and males from 165 to 622 cm (modal size class 500–549 cm). Length-at-birth for both sexes was estimated at 170 cm using a logistic regression model. Growth models for both sexes indicated a preliminary rapid growth phase followed by a second phase of slower growth. For males, a two-phase growth model also indicated a moderate growth spurt around the average age at attainment of sexual maturity (ca.12–13 years). Asymptotic lengths were estimated at 570 and 438 cm for males and females, respectively. We found strong evidence of sexual size dimorphism, with males significantly larger than females for 13 of 14 external measurements. We also found sexual dimorphism with respect to shape, with males having proportionally longer pectoral fins, wider tail flukes, and taller dorsal fins, than females. Estimates of length-at-birth, maximum ages, and sexual shape dimorphism for *G. m. edwardii* differed from those previously reported for the North Atlantic subspecies (*G. m. melas*), which may indicate subspecies or population-level differences in morphology, longevity, and sociality.

Key words: age estimation, allometry, asymptotic length, biological parameters, cetacean, growth models, life history, mass stranding, New Zealand

Accurate determination of age in marine mammals from mortality samples can contribute to reconstructing species' life histories and enabling assessment of sexual variation in ontogenetic growth patterns. Investigations of age and growth-related parameters, such as length-at-birth, growth rates, asymptotic size, sexual dimorphism, and natural longevity (maximum age), are required to allow detailed comparisons among subspecies and populations, and to assess temporal changes within populations (Stolen et al. 2002). The presence or absence of sexual dimorphism also can impart information about the life of the animal and its behavior within social groups (Shine 1989; Isaac 2005; Murphy and Rogan 2006; Mesnick and Ralls 2018). Monitoring these parameters can provide an objective means of assessing the resilience of a population to increasing

anthropogenic and environmental pressures (Caughley 1977; Evans and Hindell 2004). Such assessments are particularly important for effective conservation management of protected species such as marine mammals (Moore and Read 2008).

Historically, data used to describe external morphology and size-at-age of cetaceans were collected from whaling ships, whaling stations, and drive fisheries, primarily to assist in the management of exploited stocks (Laws 1959; Best 1970; Bloch et al. 1993a). More recently, cetacean growth has been examined using data from fisheries bycatch and stranding events (Evans and Hindell 2004; Mattson et al. 2006; Murphy and Rogan 2006; McFee et al. 2010; Ngqulana et al. 2017; Denuncio et al. 2018; Murphy et al. 2020; Plön et al. 2020). Growth models and morphological data therefore exist for many commercially exploited and bycaught species, but are unavailable for many populations, including the Southern Hemisphere subspecies of the long-finned pilot whale (LFPW; *Globicephala melas edwardii*).

Most research on the LFPW has focused on the North Atlantic subspecies (*G. m. melas*), due to extensive information provided by drive-fishery catches and mass stranding events (MSEs; Sergeant 1962a; Donovan et al. 1993). In contrast, there is a general lack of knowledge on the biological parameters of the subspecies *G. m. edwardii* throughout most of its southern range, including New Zealand. Although maximum body lengths vary geographically, male LFPWs appear to have faster growth rates and attain larger body sizes than females (Martin et al. 1987; Bloch et al. 1993a; Sigurjonsson et al. 1993). Aside from the pronounced sexual dimorphism in body size, there is some evidence of sexually dimorphic characteristics of both fins and flukes, with male LFPWs reported to have longer pectoral fins and longer and wider flukes than females of similar body lengths (Bloch et al. 1993b). It also has been suggested that dorsal fin shape differs between the sexes (Sergeant 1962b), although this has been disputed (Augusto et al. 2013). The maximum lengths and ages recorded for both male (630 cm and 46 years) and female (546 cm and 59 years) *G. m. melas* in the North Atlantic (Sergeant 1962a; Martin et al. 1987; Kasuya et al. 1988; Bloch et al. 1993a) exceed those recorded to date for male (584 cm and 31 years) and female (483 cm and 35 years) *G. m. edwardii* from the Southern Hemisphere (Crespo et al. 1985; Schroder and Castle 1998; Soto et al. 2017). Such differences in maximum length and age indicate that demographic parameters likely vary between the two subspecies.

Globicephala m. edwardii occurs year-round within New Zealand waters and frequently mass strands in high numbers on the New Zealand coast (Brabyn 1991; Berkenbusch et al. 2013; Betty et al. 2020). Here, we use data collected from MSEs on the New Zealand coast between 1948 and 2017 to empirically estimate a range of demographic parameters for *G. m. edwardii*, including: (i) length-at-birth, (ii) sex-specific growth curves, (iii) allometric relationships, and (iv) sexual dimorphism.

MATERIALS AND METHODS

Morphological data collection and validation.—This study used morphological data on LFPWs recorded in the New Zealand Whale Stranding Database (administered by the New Zealand Department of Conservation [DOC]) to December 2017. The data were checked for transcription errors and verified against original sources if these were accessible. To check measurements for transcription errors, inter-observer error (because measurements were taken by a number of different people), and outliers, regression analysis was carried out on each measurement by plotting it against total body length (TBL) for males and females separately (Murphy and Rogan 2006). Any correctly transcribed data points found to be more than 3 *SD* from the fitted line were omitted from the dataset.

The cleaned dataset of 1520 LFPWs comprised 776 females, 515 males, and 229 individuals of unknown sex, and spanned 70 years from 1948 to 2017, although most data were from carcasses stranded between 1978 and 2017 (*n* = 1512). Fifteen standard external body measurements outlined in the study by Norris (1961), as well as the sex (determined by gross examination of external genital opening) of stranded cetaceans, are routinely recorded by DOC rangers or cetacean researchers. Fourteen of these measurements are relevant to LFPWs, including nine length measurements, an axillary girth measurement, pectoral fin length and width measurements, dorsal fin height, and tail fluke width (Fig. 1). Depending on the stage of decomposition and severity of scavenger damage, not all external measurements were available for all individuals. In the case of large MSEs, often only the sex, TBL, and axillary girth, or sometimes only sex and TBL, were recorded. Sex and TBL also were recorded for 31 fetuses recovered during postmortem examinations.

Age estimation.—Of the 1,520 LFPWs examined in this study, teeth from 405 individuals (239 females, 163 males, 3 unknown sex) involved in 14 stranding events between 2006 and 2017 were collected for age estimation. Age estimation was undertaken by counting annual growth layer groups (GLGs) in decalcified and stained longitudinal sections of teeth (Perrin and Myrick 1980; Fig. 2). Tooth preparation methods for this study were adapted from Lockyer (1993). Between 3 and 10 teeth from each whale were collected from the middle of the upper or lower jaw, and either stored in 70% ethanol or frozen. Prior to processing for age determination, all teeth were catalogued, measured, and photographed with identification labels for archival reference. At least one of the least worn/damaged/curved teeth from each whale was selected, rehydrated if stored in ethanol or defrosted if frozen, and cleaned using a scalpel blade or tooth extractor. Teeth were mounted longitudinally in the centre of a slide with mounting medium (Crystalbond 509, Aremco Products Inc., New York), and ground down on both sides, using a faceting machine (Gemmasta GF4, Shell-Lap Supplies Pty. Ltd., Mile End, South Australia) equipped with a 600-grit wheel, to obtain a 3–5 mm longitudinal section through the centre of the tooth, including the crown and the root. After removal of the mounting medium, the teeth were decalcified with hydrochloric acid (RDO, Apex Engineering Products Corporation, Aurora, Illinois) until they were slightly pliable. Decalcification times ranged from four hours for teeth of neonates to ca. 24–36 h for adult teeth. Decalcified teeth were sectioned at approximately 25 µm on a carbon dioxide
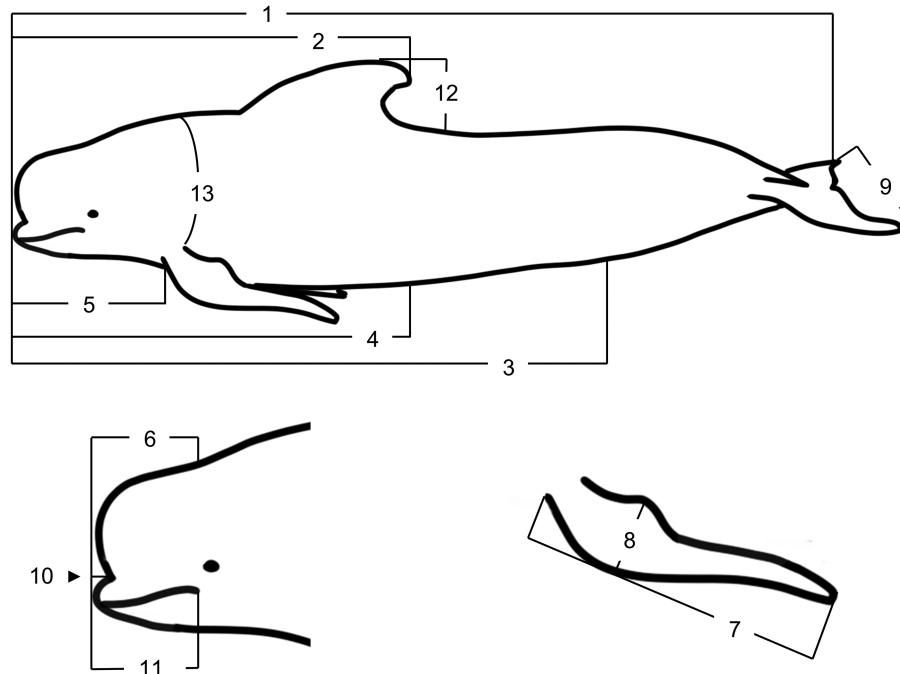
Fig. 1.—Fourteen external morphological measurements (1–13, plus length of genital slit) taken from long-finned pilot whales (*Globicephala melas edwardii*) stranded on the New Zealand coast: (1) total body length (total length; TBL); (2) tip of upper jaw to tip of dorsal fin (Ujaw dorsal), (3) tip of upper jaw to anus (Ujaw anus); (4) tip of upper jaw to genital slit (Ujaw genital); (5) tip of upper jaw to forward insertion of pectoral fin (Ujaw pectoral); (6) tip of upper jaw to blowhole (Ujaw blowhole); (7) length of pectoral fin – external (Pectoral length); (8) greatest width of pectoral fin (Pectoral width); (9) greatest width of tail flukes (Fluke width); (10) length of rostrum (Snout length); (11) tip lower jaw to corner of mouth (Ujaw gape); (12) height of dorsal fin (Height dorsal); (13) axillary girth (Axill girth); (14) length of genital slit (Genital slit).

freezing stage of a sledge microtome, using Tissue-Tek (Sakura Finetek, Torrance, California) as a mounting medium. Sections were then stained with Erlich's haematoxylin and "blued" (to fix the stain) in a weak ammonia solution. The best sections (i.e., those cut through the centre of the pulp cavity) were mounted permanently on glass slides using DPX new (Merck KGaA, Darmstadt, Germany) mounting medium.

Sections were examined under a binocular microscope for GLGs in the dentine (10–40×) and cementum (100–400×). The GLGs in the postnatal dentine were considerably more distinct than the cemental GLGs, as also noted for short-finned pilot whales (SFPW; Kasuya 2017). Assessment of GLG counts in cemental layers has previously been undertaken for LFPWs (*G. m. melas*), and they were reported to correlate to those observed in the dentine until the pulp cavity was closed or occluded (see Fig. 1 in the study by Kasuya et al. 1988). As the pulp cavity was not completely occluded in any specimen examined, GLGs in the postnatal dentine were used to assess age in this study. Dentinal GLGs were identified as consistent, adjacent incremental growth layers that included one intensely stained layer and one lightly stained layer. Accessory lines, defined as inconsistent and relatively inconspicuous layers within a GLG, also were observed frequently in the dentine. Although considered part of the GLG pattern, the accessory lines were identified to ensure they were not included in GLG counts.

All sections were read by two or three individuals, including at least one expert reader (E.L.B. or S.M.). Readers evaluated the tooth sections three times independently, without prior knowledge of body length or sex, and then compared assessments to assign the best age estimate or an age range for each animal based on Hohn and Fernandez (1999). If readers disagreed on the age, the sections were examined again. If the difference was higher than one GLG, all readers re-read the tooth, and if no agreement was reached, another tooth was sectioned and read by all readers. If the increments still were difficult to count on the second tooth, all readers discussed the interpretation and either reached an agreed age or judged the tooth to be unreadable. Individuals for which age could not be estimated reliably were excluded from further analysis. Calves that did not possess a neonatal line in the tooth, or had a neonatal line forming, with no additional postnatal dentine, were classified as newborns.

Length-at-birth.—The probability of birth (p) as a function of TBL was modeled using a Bayesian logistic regression with "HOF" parameterization (Huisman et al. 1993), as follows:

$$y_i \sim \text{Bernoulli}(p_i)$$

$$\log\left(\frac{p_i}{1 - p_i}\right) = \omega(x_i - l_{50})$$

where i indexes individuals, y_i either is 0 (unborn) or 1 (born), x_i gives the lengths of individuals. The two model parameters are l_{50}, giving the median length-at-birth (i.e., the length at which the probability of birth is 50%), and ω, which is a rate parameter. All Bayesian
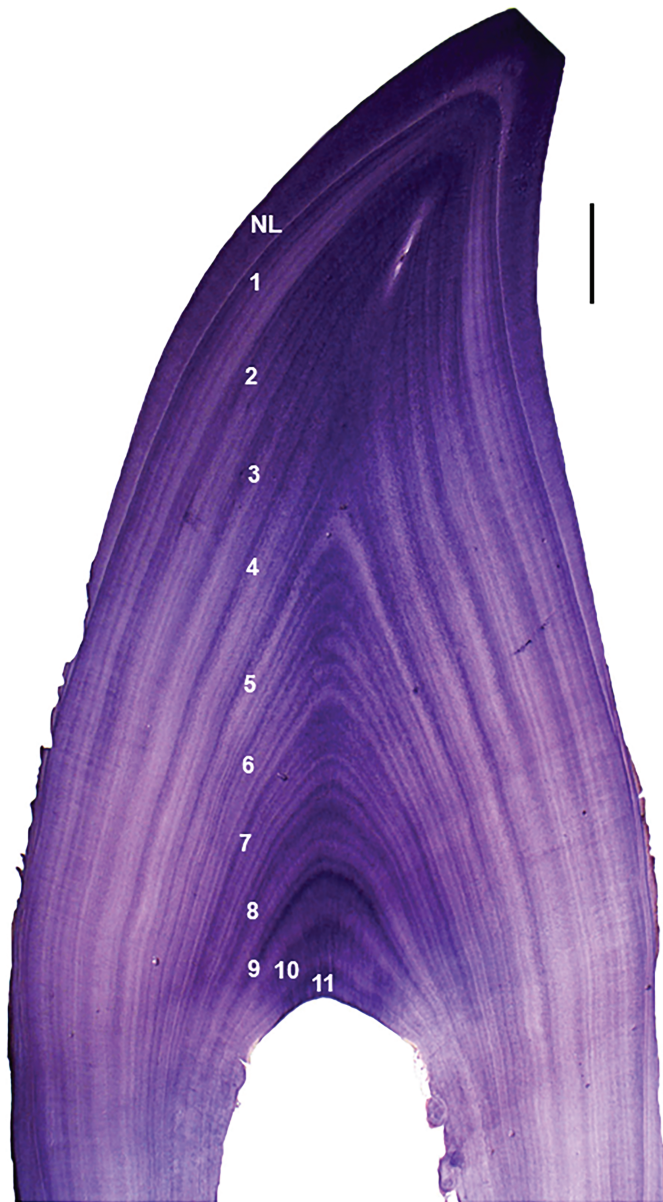
Fig. 2.—Growth layer groups (GLGs) in the dentine of a male long-finned pilot whale (*Globicephala melas edwardii*; GM46) stranded on the New Zealand coast in 2009 and aged 11 years. NL = neonatal line. Scale bar = 1 mm. Note open pulp cavity and presence of accessory lines within GLGs.

models were fitted using Stan (Stan Development Team 2021) in R (R Development Core Team 2021). See Supplementary Data SD1 for Stan code. After prior predictive simulation (Supplementary Data SD2), the weakly informative priors were chosen for model parameters $l_{50} \sim N(171, 20)$ and $\omega \sim N^{+}(0, 1)$. This model was fitted to a dataset of all fetuses and postnatal whales ≤300 cm ($n = 202$) for which TBL measurements were available. Of these, $n_0 = 31$ were unborn and $n_1 = 171$ were born. To mitigate the effects of the unbalanced sample on estimates (Salas-Eljatib et al. 2018), weights were assigned to each case from group k according to the sample size of the group, n_k, relative to the overall sample size, n, using $w_k = \sqrt{0.5/(n_k/n)}$. The vector of weights w_i was then normalized to have an average of 1.

Additional logistic regression models were fitted to evaluate the difference in the median lengths-at-birth (l_{50}) between males and females. Individuals with unknown sex were excluded for this analysis, reducing the overall sample size from 202 to 169. Born and unborn samples were weighted using the equation for w_k above, but with weights calculated separately for each sex. Two models were fitted: one with and one without different estimates of l_{50} for the sexes. These two models were compared using Leave-One-Out Information Criterion and model weights (LOOIC; with Pareto-smoothed importance sampling and refitting models for observations with Pareto $k > 0.7$; see the "loo" package for R; Vehtari et al. 2017, 2020). Posterior distributions for quantities of interest were summarized with means and 95% highest posterior density intervals (HPDI).

Two additional statistics were calculated to enable comparisons with previously published length-at-birth estimates for the northern subspecies of LFPW (*G. m. melas*): (i) mean-overlap—the mean of overlapping fetal and calf lengths by including the values of the largest non-overlapping fetus and the smallest non-overlapping calf (Bloch et al. 1993a, Börjesson and Read 2003); (ii) mean neonatal length—the mean length of calves that did not possess a neonatal line in the tooth or had a neonatal line forming, with no additional postnatal dentine, i.e., classified as a newborn (Kasuya and Marsh 1984, Bloch et al. 1993a, Murphy et al. 2009). The difference in the mean-overlap statistic between males and females was tested using a Student's *t*-test.

Growth models.—Several growth curves were considered with the primary focus on sex-specific von Bertalanffy and Gompertz models fitted to the age-length data. The von Bertalanffy and Gompertz growth models have been used to model growth in many cetacean species, including pilot whales (Bloch et al. 1993a). The von Bertalanffy model (von Bertalanffy 1938; Bloch et al. 1993a) is as follows:

$$L_t = A\left[1 - b \cdot \exp\left(-kt\right)\right]$$

and the equation for the Gompertz growth model (Laird 1966; Fitzhugh 1976; Bloch et al. 1993a) is:

$$L_t = A\left\{\exp\left[-b \cdot \exp\left(-kt\right)\right]\right\}$$

where L_t is the TBL at age (t), A is the asymptotic value, b is the constant of integration, and k is the growth rate constant.

Both these models limit growth to a monotonically decreasing function and cannot represent multiple phases of growth. Using the equations above, two-phase von Bertalanffy and Gompertz growth models (Perrin et al. 1976) also were used to simultaneously fit separate equations to the age-at-length data, using an iterative least-squares method. The two-phase model was used to account for the secondary growth spurt observed in many delphinids (Perrin et al. 1976; Murphy et al. 2009; McFee et al. 2010; Jefferson et al. 2012; Agbayani et al. 2020). The intersection point of the two models was estimated as the age at which the total sum of squares for the fit of both models was the smallest (Perrin et al. 1976; Danil and Chivers 2007). Growth curve parameters for the models were estimated and the most

appropriate model selected using the Akaike information criterion (AIC).

Allometry.—To analyze growth patterns and compare them between the sexes, allometric growth equations for 13 measurements were created in the form:

$$y = ax^b$$

where *y* is the measurement (dependent variable), *x* is the TBL (independent variable), *b* is the growth coefficient, and *a* is the intercept (Schmidt-Nielsen 1993). Negative allometry is indicated when the growth coefficient is significantly <1, positive allometry is indicated when the growth coefficient is significantly >1, and isometric allometry is indicated when the coefficient is not significantly different from 1 (Read and Tolley 1997). To test the null hypothesis $H_0 : b = 1$, the test statistic (t_s) was calculated as

$$t_s = \frac{b - 1}{SE_b}$$

where b = slope, SE_b = standard error of slope, $d.f. = n - 2$ and $\alpha = 0.05$, using Student's *t*-test tables. Comparing slope analysis was undertaken to compare growth coefficient values between male and female pilot whales, d.f. $= n - 4$ and $\alpha = 0.05$, using Student's *t*-test tables. Data were used from all physically immature and mature pilot whales and no post hoc adjustments were made to *P*-values.

Sexual dimorphism.—Sexual dimorphism was investigated only in physically mature individuals (defined as TBL ≥ 0.9 ×asymptotic length, to account for the lack of clear asymptote in the male growth data). Following Murphy and Rogan (2006), dimorphism was measured in two ways: sexual size dimorphism without correcting for body size; and sexual shape dimorphism, to account for variations in body length. Sexual size dimorphism investigates overall variations in body size and differences in shape. Sexual shape dimorphism investigates the differences in shape only, i.e., the relative size of a body part. The relationships between sex and morphological measurements were explored using charts and Spearman's rank correlation coefficients. Morphological data from all physically mature males and females were tested for normality (Shapiro–Wilk test) and homogeneity of variance (Levene's test) before analysis.

Each morphological measurement was analyzed separately for males and females by carrying out Welch's univariate analysis of variance (ANOVA) and univariate analysis of covariance (ANCOVA). Welch's ANOVA was used to investigate size and shape variation between the sexes. Using TBL as the covariate, ANCOVA removed the effect of body size on individual measurements and investigated sexual variations of body shape only. Because testing suggested a departure of data from normality, all morphological data were transformed to a logarithmic scale $[\log_{10}(x)]$ prior to ANCOVA analysis. The tip of the upper jaw to genital slit measurement (Ujaw genital) was excluded from ANCOVA analysis due to the differing position of the genital slit between the sexes. The length of rostrum measurement (Snout length) also was excluded from ANCOVA because it was not found to have a linear relationship with TBL. No post hoc adjustments were made to *P*-values.

If individuals were missing more than five measurements, they were eliminated from the dataset used for multivariate analysis. The remaining missing variables were calculated using multiple imputation (linear regression method). The resulting dataset was used to carry out linear discriminant function analysis to investigate sexual dimorphism in body size and shape. Insufficient sample sizes were available for the following measurements, and they were omitted from the analysis: length of rostrum (Snout length) and length of genital slit (Genital slit). The tip of upper jaw to genital slit measurement (Ujaw genital) also was excluded from multivariate analysis due to the differing position of the genital slit between the sexes.

RESULTS

Body length and age.—TBL for the entire sample ranged from 160 to 622 cm ($n = 1,520$), with a modal size class of 400 to 449 cm (median 423; Fig. 3). Where sex was reported, females and males ranged in TBL from 160 to 500 cm ($n = 776$), and from 165 to 622 cm ($n = 515$), respectively. Age was estimated for 384 LFPWs measuring from 176 to 485 cm for females ($n = 227$) and 180 to 622 cm for males ($n = 154$). Age ranges or a minimum age were obtained from a further 22 whales (all > 15 years) due to difficulties in counting GLGs in their dentine. Females ranged from 0 to 38 years, and males from 0 to 31 years, with 99% of the aged sample sexed.

Length-at-birth.—A total of 31 fetuses were recorded during postmortem examinations, measuring between 5 and 176 cm in TBL. The smallest male and female calves (confirmed live born via field observations) measured 165 and 160 cm TBL, respectively, and the largest fetuses of both sexes measured 176 cm. Overall, there were seven fetuses and 15 neonates measuring between 160 and 176 cm TBL. The results for each of the statistics used to compare estimated length-at-birth are summarized in Table 1.

The overall median length-at-birth is estimated to be 170.4 cm (posterior mean; 95% HPDI = 164.7, 175.6), based on a logistic regression of data from all males, females, and unknown sex cases with length ≤ 300 cm ($n = 202$; Fig. 4). The comparison of models of males and females only ($n = 169$) provided no support for any substantial difference in length-at-birth between the sexes. The posterior distribution of the difference was centered near zero, with males very slightly longer on average (median difference = 2.6 cm, 95% HPDI = −9.0, 14.5; see Supplementary Data SD3). The LOOIC weights of the models with and without a difference between sexes were 0.0 and 1.0, respectively, indicating that sex did not improve the models' ability to discriminate between born and unborn calves based on their lengths.

The additional two statistics (mean-overlap and mean neonatal length) were calculated for comparison with the northern subspecies (*G. m. melas*) in other studies. Using the
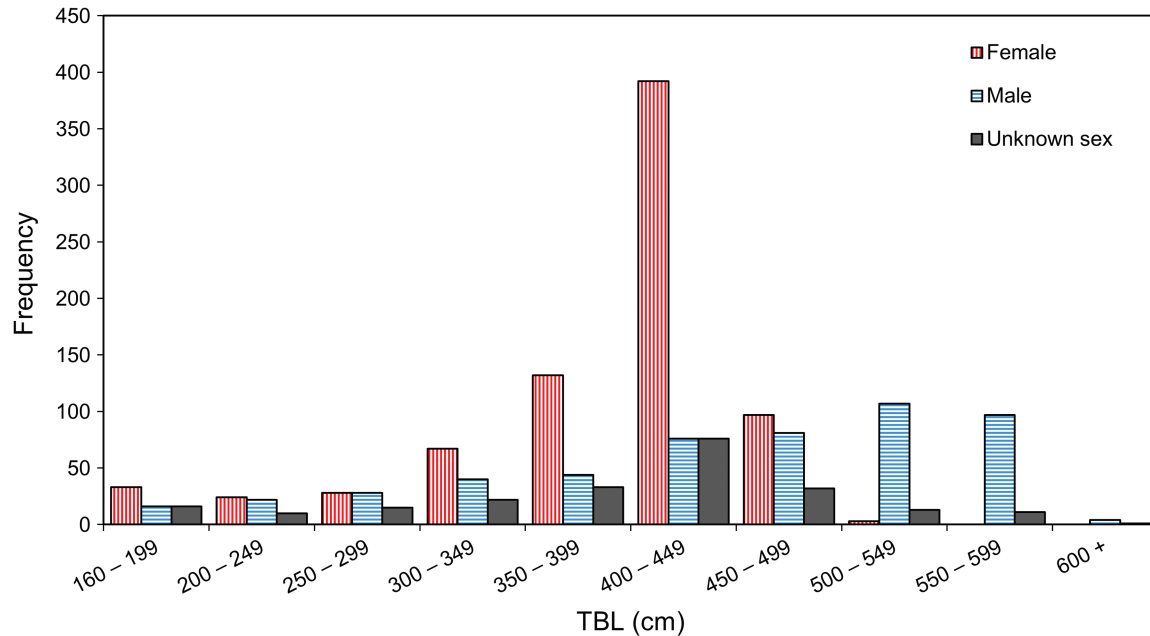
Fig. 3.—Length–frequency distributions for female ($n = 781$), male ($n = 523$), and unknown sex ($n = 230$) long-finned pilot whales (*Globicephala melas edwardii*) stranded on the New Zealand coast between 1948 and 2017.

Table 1.—Estimated length-at-birth (cm) of long-finned pilot whales (*Globicephala melas edwardii*) in New Zealand waters, calculated using three different methods.

Method	n	Estimate	95% interval
Logistic regression	202	170	165–176
Mean overlap	22	171	169–173
Mean neonatal length	6	182	175–188

The logistic regression estimate for the full dataset (males, females, and unknown sex) is considered the best estimate of length-at-birth for long-finned pilot whales in New Zealand waters. The estimate and 95% interval from the logistic regression model is the mean and highest posterior density interval from the posterior distribution of the median length-at-birth (i.e., the length at which the probability of birth is 50%); for the other methods, standard means and 95% confidence intervals are reported.

mean-overlap statistic, no significant difference was found between the estimated length-at-birth for males and females ($t = 1.39$; $P = 0.19$). The pooled estimate for males and females combined was 171 cm (95% CI = 169–173 cm, $n = 22$). Because it is based on naïvely taking the average length from all postnatal and prenatal specimens that fall within the overlap criteria, this method is expected to be sensitive to having an unbalanced sample. In the current dataset, although there were substantially more postnatal than prenatal measurements available, the average of the overlapping lengths was similar to the estimated median length-at-birth obtained from the weighted logistic regression (170.4 cm). For the mean neonatal length statistic, the dataset comprised five newborn females and one newborn male with no neonatal line. Given such small sample sizes, only the pooled estimate of average length-at-birth of 182 cm (95% CI = 175–188 cm, $n = 6$) was calculated. This method is expected to overestimate length-at-birth because it includes only postnatal animals. Given the known caveats of the

mean overlap and mean neonatal length methods, the weighted HOF logistic regression method is preferred for estimating length-at-birth. The logistic regression method is able to include both pre- and postnatal data and also has the advantage of being able to define any quantity of interest (e.g., l_{50} and the difference in l_{50} between sexes) and summarize the plausible values of such quantities using a posterior distribution.

Growth.—Significant postnatal sexual size dimorphism was evident; separate growth curves therefore were created for males and females, with individuals of unknown sex omitted from the models. Gompertz and von Bertalanffy equations were used to describe growth in both male and female LFPWs, with the von Bertalanffy model providing a better fit for both males and females, based on AIC scores (Table 2). The points of intersection at the *y*-axis were determined by selecting the curves that best fitted the dataset.

In the first 5 years of growth, the TBL both of females and males increased rapidly (Fig. 5). Using the single von Bertalanffy model, females continued to grow rapidly (41 cm year^{-1} in their first, 20 cm year^{-1} in their fifth year) until they reached a TBL of 400 cm at approximately 10 years of age. After age 10, the rate of growth slowed to 7 cm year^{1}, and then to less than 1 cm year^{1} by 22 years of age and approximately 434 cm in length (Figs. 5 and 6). The asymptotic value obtained for female TBL was 438 cm (Table 2; Fig. 5). In this study, individuals that attained a TBL of $0.9 \times$ the mean asymptotic length were considered physically mature; for females, this is 394 cm in length, and 10 years in age.

Following the initial growth spurt of 45 cm year^{-1} in their first year to 21 cm year^{-1} in their fifth year, male LFPWs appear to undergo a second growth spurt at around 12 to 13 years of age and continue to grow for a longer period than females (Fig. 6). For males, a two-phase von Bertalanffy model was used to
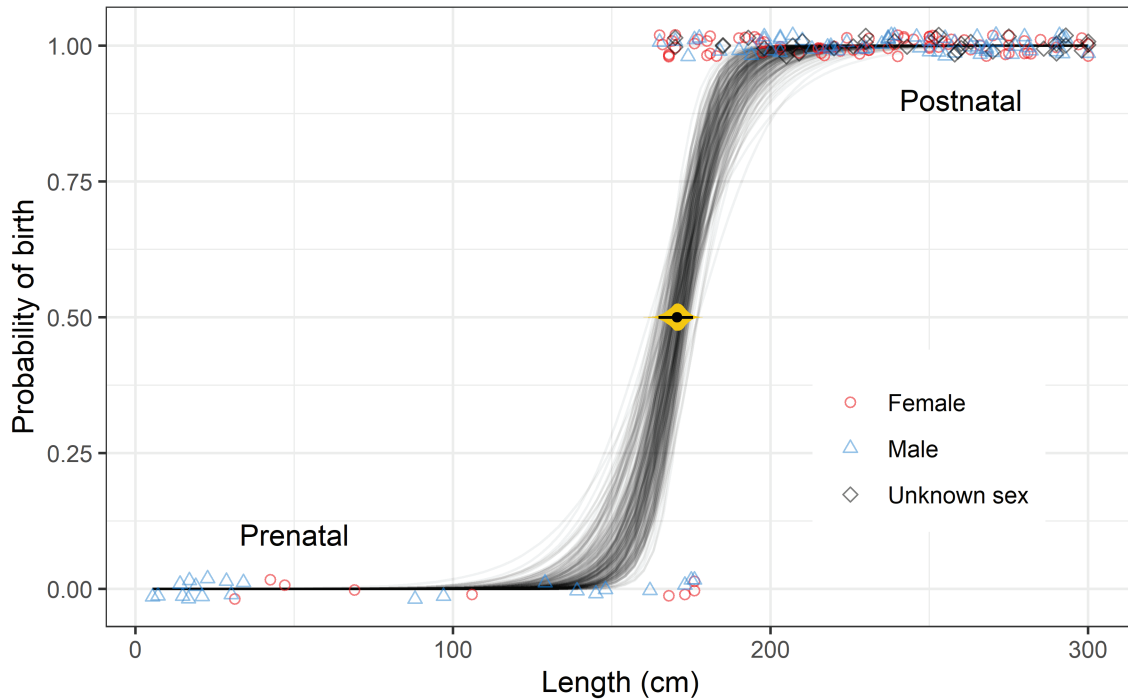
Fig. 4.—The lengths of pre- and postnatal long-finned pilot whales (*Globicephala melas edwardii*; points) stranded on the New Zealand coast (1948–2017), with a posterior sample of 200 logistic curves for the probability of birth as a function of length (thin grey lines) using a model that disregarded sex, fitted to $n = 202$ cases. A small amount of transparency and vertical "jitter" was added to help visualize overlapping points. The central black point and thin horizontal line show the mean and 95% highest posterior density interval for the estimated median length-at-birth (i.e., the length at which the probability of birth is 50%), with gradient plot in yellow (Kay 2021).

Table 2.—Estimated growth parameters, 95% confidence intervals (CI) and Akaike information criterion (AIC) scores for the Gompertz and von Bertalanffy growth curves derived from male (M) and female (F) long-finned pilot whales (*Globicephala melas edwardii*) stranded on the New Zealand coast (2006–2017).

Model	A (95% CI) F	A (95% CI) M	B (95% CI) F	B (95% CI) M	k (95% CI) F	k (95% CI) M	AIC score F	AIC score M
Single Gompertz	435.5	602.0	0.76	0.96	0.23	0.11	1759.49	1795.01
	(430.9–440.2)	(573.5–630.5)	(0.72–0.81)	(0.91–1.01)	(0.21–0.25)	(0.09–0.13)		
Two-phase Gompertz (<13 years)		453.5		0.78		0.25		1770.96
		(434.5–472.5)		(0.72–0.83)		(0.20–0.30)		
Two-phase Gompertz (>13 years)		569.2		3.05		0.22		1770.96
		(531.6–606.8)		(−4.53–10.63)		(0.02–0.42)		
Single von Bertalanffy	438.4*	633.9	0.55	0.65	0.19	0.07	1753.69	1790.10
	(433.3–443.5)	(592.1–674.9)	(0.53–0.57)	(0.63–0.67)	(0.17–0.20)	(0.06–0.09)		
Two-phase von Bertalanffy (<13 years)		465.2		0.56		0.19		1770.11
		(440.1–490.2)		(0.54–0.59)		(0.14–0.24)		
Two-phase von Bertalanffy (>13 years)		570.0*		2.38		0.20		1770.11
		(530.8–609.1)		(−3.41–8.17)		(0.01–0.40)		

*The single- (female) and two-phase (male) von Bertalanffy models are considered to provide the best estimates of asymptotic length for long-finned pilot whales in New Zealand waters.

account for the apparent growth spurt around the average age at attainment of sexual maturity (13.5 years; Betty et al. 2019). The two-phase model provided a significantly better fit than the single von Bertalanffy model for the male data—although the two-phase Gompertz model also provided a good fit (Table 2; Fig. 5). Using the two-phase von Bertalanffy model, the estimated inflection point (i.e., growth spurt, increasing from 6 to 35 cm year⁻¹) for male LFPWs occurred at approximately 13 years in age and 438 cm in TBL. After this point, rapid growth continues until they reach a length of approximately 517 cm at 16 years of age, followed by a period of slower growth—decreasing from 10 cm year⁻¹ to less than 1 cm year⁻¹ by 29 years of age and a TBL of approximately 566 cm (Figs. 5 and 6). In this study, male growth did not clearly reach the estimated asymptotic length of 570 cm but continued to grow slowly with age; physical maturity (TBL of 0.9 × asymptotic
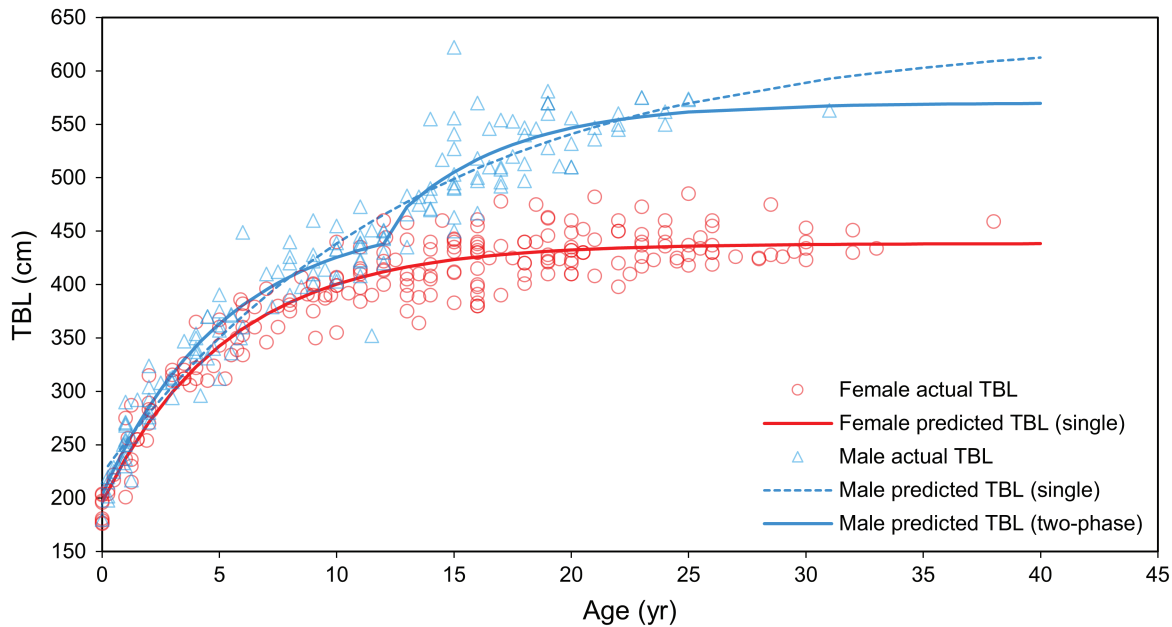
Fig. 5.—Von Bertalanffy growth curves superimposed on length-at-age data for female ($n = 220$) and male ($n = 154$) long-finned pilot whales (*Globicephala melas edwardii*) stranded on the New Zealand coast (1948–2017). Note: Male total body length (TBL) does not appear to reach an asymptote when growth is modeled using a single growth curve.

length) is considered to be attained at 513 cm in length and 16 years in age.

Allometry.—Significant allometry was observed for 10 out of 13 and 11 out of 13 morphological measurements in females and males, respectively, which is more than expected to be significant by chance (5%). Nearly all linear body measurements (Ujaw dorsal, Ujaw anus, Ujaw genital, Ujaw pectoral, Ujaw blowhole, Snout length, Ujaw gape, Genital slit; see Fig. 1) were negatively allometric in both male and female LFPWs, except genital slit length which exhibited isometric growth in females (Table 3). The growth coefficients for the length of the genital slit ($t = 1.923$, d.f. = 110, $P = 0.044$) provided evidence that females have a higher growth rate for this measurement than males. The axillary girth measurement exhibited isometric growth in males and was negatively allometric in females, although there was no significant variation in the growth rate for this measurement between males and females ($t = 1.726$, d.f. = 341, $P = 0.085$). Pectoral fin width was negatively allometric in growth in both sexes. However, pectoral fin length and fluke width were isometric in females, but positively allometric in males. In females, the height of the dorsal fin exhibited negative allometric growth, whereas in males it was isometric in growth. Significant variation was evident between the sexes for 5 out of 13 body measurements, which is more than expected to be significant by chance (5%). In particular, sexual variation was evident in the allometry of appendage measurements, with males having a higher growth rate than females (Table 3); i.e., in order of decreasing level of significance, fluke width ($t = 4.248$, d.f. = 385, $P < 0.001$), pectoral fin length ($t = 2.428$, d.f. = 478, $P = 0.016$), pectoral fin width ($t = 2.272$, d.f. = 274, $P = 0.024$), and height of dorsal fin ($t = 2.028$, d.f. = 279, $P = 0.044$).

Sexual dimorphism.—The mean ($\bar{x}$), standard error (*SE*), and range, for external measurements in physically mature (i.e.,

TBL ≥ 0.9 × asymptotic length) LFPWs are indicated in Table 4. The mean lengths obtained for physically mature males and females were 550 and 432 cm, respectively, giving a sexual size dimorphism (SSD) ratio of 1.27. As observed in Supplementary Data SD4 and SD5, considerable sexual dimorphism is evident in all external measurements, except genital slit length, with males particularly discriminated from females by TBL and pectoral fin length.

Sexual size dimorphism also was evident in physically mature LFPWs when tested using Welch's ANOVA. TBL and 12 of 13 other external measurements exhibited sexual size dimorphism (variation in body size and/or body shape), more than expected to be significant by chance (5%). Male LFPWs were significantly larger in all measurements, except the length of the genital slit (14_Genital_slit; Table 4). However, only 3 out of 11 measurements (still more than the 5% expected by chance) were sexually shape dimorphic, with males having considerably longer pectoral fins, taller dorsal fins, and wider tail flukes than females (in order of decreasing level of significance), irrespective of TBL (Table 4).

Linear discriminant analysis was used to examine differences between males and females with respect to a linear combination of 11 morphological measurements. A single discriminant function accounted for 100% of the sexual dimorphism observed (using pooled multiple imputation data: Wilk's $\lambda = 0.110$, $\chi^2 = 371.457$, d.f. = 11, canonical correlation = 0.943, $P < 0.001$). The standardized canonical discriminant function coefficients for the 11 morphological measurements are listed in Table 4. Functions at the group centroids were −1.804 for females and 4.421 for males, using pooled multiple imputation data. Reclassification of cases based on the new canonical function was highly successful: 100% of the cases were correctly reclassified into their correct sex.
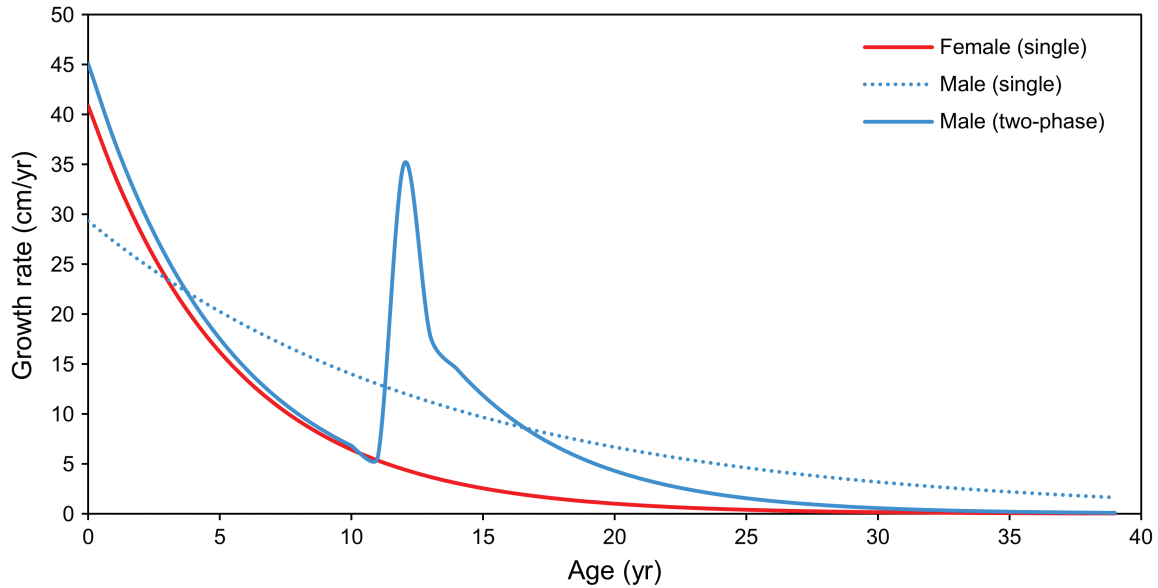
Fig. 6.—Estimated growth rates (cm/year) for male (n = 153) and female (n = 220) long-finned pilot whales (*Globicephala melas edwardii*) stranded on the New Zealand coast (1948–2017) as estimated from single (male and female) and two-phase (male) von Bertalanffy growth models. Note: Secondary growth spurt in males, observed in the two-phase model, estimated to occur at approximately 13 years of age.

Table 3.—Allometric growth relationships for 13 external body measurements regressed against total body length (TBL) for both female (F) and male (M) long-finned pilot whales (*Globicephala melas edwardii*) stranded on the New Zealand coast (1948–2017).

Measurement	Female	SE (b)	n	r^2	b	Male	SE (b)	n	r^2	b	F vs. M
2 Ujaw dorsal	$y = 1.104x^{0.874}$	0.010	289	0.961	<1	$y = 1.243x^{0.854}$	0.010	202	0.975	<1	ns
3 Ujaw anus	$y = 0.775x^{0.964}$	0.010	198	0.980	<1	$y = 0.822x^{0.955}$	0.012	128	0.980	<1	ns
4 Ujaw genital	$y = 0.782x^{0.946}$	0.012	296	0.951	<1	$y = 0.781x^{0.933}$	0.015	207	0.951	<1	ns
5 Ujaw pectoral	$y = 0.971x^{0.703}$	0.014	344	0.884	<1	$y = 1.031x^{0.692}$	0.015	245	0.901	<1	ns
6 Ujaw blowhole	$y = 0.760x^{0.657}$	0.025	281	0.712	<1	$y = 0.922x^{0.630}$	0.024	211	0.768	<1	ns
7 Pectoral length	$y = 0.187x^{1.006}$	0.018	291	0.917	ns	$y = 0.130x^{1.071}$	0.020	191	0.937	>1	F < M
8 Pectoral width	$y = 0.116x^{0.872}$	0.019	160	0.930	<1	$y = 0.080x^{0.938}$	0.022	118	0.939	<1	F < M
9 Fluke width	$y = 0.189x^{1.020}$	0.017	234	0.936	ns	$y = 0.092x^{1.144}$	0.023	155	0.940	>1	F < M
10 Snout length	$y = 0.272x^{0.410}$	0.136	139	0.063	<1	$y = 0.213x^{0.412}$	0.124	75	0.131	<1	ns
11 Ujaw gape	$y = 0.474x^{0.691}$	0.041	191	0.599	<1	$y = 1.133x^{0.546}$	0.035	131	0.657	<1	ns
12 Height dorsal	$y = 0.172x^{0.823}$	0.041	168	0.707	<1	$y = 0.094x^{0.933}$	0.036	115	0.858	ns	F < M
13 Axill girth	$y = 0.964x^{0.903}$	0.028	207	0.839	<1	$y = 0.620x^{0.974}$	0.030	138	0.884	ns	ns
14 Genital slit	$y = 0.099x^{0.977}$	0.103	71	0.566	ns	$y = 0.936x^{0.614}$	0.158	43	0.269	<1	F > M

Growth patterns have been determined in the form of $y = ax^b$, where x = TBL (cm); y = measurement (cm); b = growth coefficient; a = intercept. *SE* = standard error for growth coefficient; n = sample size; r^2 = correlation coefficient; F vs. M, comparison of slopes between sexes with TBL as the independent variable; ns = no significant evidence ($P > 0.05$) that $b \neq 1$, or F ≠ M. For explanation of measurement codes see Fig. 1.

DISCUSSION

Age estimation.—This study presents the maximum recorded ages for *G. m. edwardii* in New Zealand waters as 31 years for males and 38 years for females. These maximum ages are considerably lower than those reported for *G. m. melas* sampled from drive fisheries in both Newfoundland (male: 35 years, female: 56 years; Sergeant 1962a; Kasuya et al. 1988) and the Faroe Islands (male: 46 years, female: 59 years; Bloch et al. 1993a; Table 5), and also those reported from SFPWs captured in the Japanese fishery (male: 46 years, female: 64.5 years; Kasuya and Marsh 1984; Kasuya and Matsui 1984; Kasuya and Tai 1993). However, they are similar to the maximum ages reported for stranded *G. m. melas* in the North Atlantic (male and female: 34 years; Martin et al. 1987; Sigurjonsson et al. 1993). These differences in maximum ages between the present and past studies could be explained in any one or more of three ways: (i) older animals are present in the Southern Hemisphere subspecies under study here, but they are less likely to strand *en masse* or their carcasses were not recovered or aged; (ii) errors in age estimation resulting in an underestimate of the true age of the stranded animals; or (iii) species, subspecies, and population-level differences in pilot whale longevity.

First, lower estimates of LFPW longevity from stranding-based studies (in both subspecies; Table 5) could reflect the fact that they were based on smaller sample sizes than drive fishery-based studies. Stranded groups may represent sub-groups rather than the entire pod, resulting in older individuals being missed in the sample by chance. It also is possible that older individuals are less likely to strand *en masse*, or more likely to survive stranding events and so therefore were not sampled. In this

Table 4.—Mean ($\bar{x}$, standard error (*SE*), range and sample size (*n*) of 14 morphological measurements, with results of Welch's ANOVAs, ANCOVAs, and multivariate linear discriminant analysis comparing data collected from physically mature male and female long-finned pilot whales (*Globicephala melas edwardii*) stranded on the New Zealand coast (1948–2017).

	Female				Male				ANOVA	ANCOVA	SCDFC
	$\bar{x}$ (cm)	±*SE*	Range (cm)	*n*	$\bar{x}$ (cm)	±*SE*	Range (cm)	n	*P*	*P*	
1 Total length (TBL)	431.9	0.9	394–500	519	550.0	1.5	513–622	188	***	na	0.801
2 Ujaw dorsal	220.2	0.9	186–250	184	270.9	1.7	242–300	71	***		−0.178
3 Ujaw anus	273.4	1.1	246–300	119	333.2	2.8	296–370	43	***		0.056
4 Ujaw genital	240.2	1.0	203–285	186	272.8	2.1	246–330	64	***	na	na
5 Ujaw pectoral	68.1	0.3	55–83	216	78.5	0.7	66–99	80	***		−0.026
6 Ujaw blowhole	40.2	0.3	31–54	176	47.2	0.6	36–60	68	***		0.109
7 Pectoral length	85.5	0.5	70–107	183	113.7	1.1	85–132	67	***	***	0.275
8 Pectoral width	23.1	0.2	19–28	87	30.1	0.5	25–36	38	***		−0.041
9 Fluke width	92.2	0.6	70–108	139	125	1.5	94–150	53	***	*	0.161
10 Snout length	3.9	0.2	1–10	80	3.1	0.3	1–6	26	**	na	na
11 Ujaw gape	30.4	0.4	19–38	113	34.7	0.7	26–42	48	***		−0.040
12 Height dorsal	25.4	0.4	16–33	91	34.6	0.8	22–47	38	***	**	0.127
13 Axill girth	230.3	2.6	188–320	125	285.2	5.5	216–360	44	***		−0.032
14 Genital slit	37.4	1.6	19–62.5	37	42.1	4.4	22–75	14			na

SCDFC = standardized canonical discriminant function coefficients, na = not analyzed, *P < 0.05, **P < 0.01, ***P < 0.001. M > F for all sexually dimorphic measurements. For explanation of measurement codes see Fig. 1

study, age and TBL were not always determined for all individuals in large MSEs. Some older animals therefore may have been missed in the sampling process (see Fig. 3). While this factor cannot be ignored, this study is based on a large, minimally biased sample (i.e., particular ontogenetic groups were not favored, except two out of 12 MSEs where adult males were targeted for gonadal sampling; see Betty et al. 2019) that likely reflects the true age distribution of the MSEs, and also the local New Zealand population (Betty 2019). In a New Zealand context, mass-stranded LFPW groups are biased towards females, particularly within the adult age-classes, while a male bias is reported in juveniles (Betty 2019; Betty et al. 2020). The bias towards females in the sex ratio of adult animals also is reflected in drive fishery catches of the northern subspecies and probably is explained by the higher male mortality rates described for both *G. m. edwardii* (Betty et al. 2020) and *G. m. melas* (Martin et al. 1987; Bloch et al. 1993a; Desportes et al. 1994) or possible adult male emigration from natal groups for breeding purposes (Desportes et al. 1993).

Second, the lower maximum ages reported in this study (and other stranding-based studies; e.g., Martin et al. 1987; Sigurjonsson et al. 1993), compared with those reported in LFPWs sampled in Newfoundland (Kasuya et al. 1988) and the Faroe Islands (Bloch et al. 1993a), may reflect the fact that cemental readings were not used in this study. Lockyer et al. (1987) and Kasuya et al. (1988) found a strong correlation in dentinal and cemental GLGs from the teeth of LFPWs up to around 14 years of age in individuals with open or closing pulp cavities. Beyond this age, the correlation was substantially weakened, with the number of cemental layers often greater than those observed in the dentine when the pulp cavity was closed/occluded (see Fig. 1 in Kasuya et al. 1988). In the current study, only growth layer counts from the dentine were used for age estimation because the readability of the cemental layers was considered inferior, as also reported for SFPWs (Kasuya

2017). Although the pulp cavities were undoubtedly still open in the oldest animals sampled, it was not possible to prove or disprove that readable dentine still is being deposited in the oldest LFPWs in the New Zealand sample. The close similarity between the growth curves derived by Kasuya et al. (1988) and Bloch et al. (1993a), based on dentinal and cemental layers, and those based only on dentinal counts in this study (Fig. 5) suggests that the latter age estimates are reliable. Nevertheless, given the degree of uncertainty of age estimates for teeth where the pulp cavity is almost occluded, as well as the higher incidence of tooth anomalies in individuals older than 15 years, it perhaps is prudent to follow Martin et al. (1987) in considering age estimates for older animals (> 20yrs) as a minima.

Finally, while acknowledging potential caveats associated with sampling from stranding events compared with drive fisheries, and age estimation using dentinal *vs.* cemental growth layers, ages of the oldest specimens of the southern subspecies *G. m. edwardii* sampled to date were younger than those of the northern subspecies *G. m. melas* by 21 years in females and by 15 years in males (see Table 5). The potential difference in longevity between the two subspecies is supported by estimates of other life history parameters, where *G. m. edwardii* attains sexual maturity at a younger age (on average 6.7 years for females, 13.5 years for males; ages before dentine-only ageing would be an issue) and smaller body size, which jointly may suggest a higher mortality rate in the southern subspecies (Betty 2019, Betty et al. 2019).

Length-at-birth.—Methods previously used to estimate length-at-birth were applied to allow comparisons with previous studies of *G. m. melas* in the North Atlantic. Using a comparable method to our preferred method (logistic regression), Bloch et al. (1993a) reported a considerably larger median length-at-birth (177 cm) for *G. m. melas* off the Faroe Islands than estimated for LFPWs off New Zealand (*G. m. edwardii*; 170 cm). The mean-overlap statistic also was applied to *G. m. melas* by

Table 5.—Total body length (TBL) and age data available for long-finned pilot whales (*Globicephala melas*) from various geographical areas.

		Globicephala melas melas				Globicephala melas edwardii	
Location		Britain[1]	Faroe Islands[2,3]	Iceland[4]	Newfoundland[5,6]	Argentina[7,8]	New Zealand[9]
Source		Stranding	Drive fishery	Stranding	Drive fishery	Stranding	Stranding
Sampling period		1982–1985	1986–1992	1982–1986	1951–1959	1982, 2009	1948–2017
Length-at-birth (cm)			177[a]		M: 178[b]		170[a]
			(n = 143)		(n = 59)		(n = 202)
					F: 174[b]		
					(n = 49)		
Asymptotic length (cm)	M	550–600[c]	580[d]		557[e]		570[g]
		(n = 21)	(n = 965)		(n = 5)		(n = 154)
	F	400 – 450[c]	445[d]		489[e]	441[f]	438[f]
		(n = 31)	(n = 1,478)		(n = 53)	(n = 31)	(n = 227)
Age at asymptotic length (years)	M	>20[h]	>46		21–25[i]		40
		(n = 21)	(n = 965)		(n = 152)		(n = 154)
	F	>20[h]	32		21–25[i]		30
		(n = 31)	(n = 1,478)		(n = 275)		(n = 227)
Maximum length (cm)	M	630	625	595	617	538	622
			(n = 1,190)	(n = 55)	(n > 1,275)	(n = 7)	(n = 515)
	F	546	512	475	511	483	500
			(n = 1,635)	(n = 119)	(n > 1,951)	(n = 62)	(n = 776)
Maximum age (years)	M	20[h]	46	34	35.5[i]	16	31
		(n = 21)	(n = 967)	(n = 38)	(n = 153)	(n = 5)	(n = 154)
	F	25[h]	59	34	56.5[i]	35	38
		(n = 31)	(n = 1,482)	(n = 92)	(n = 284)	(n = 40)	(n = 227)

[a]Length-at-birth estimated by logistic regression.
[b]Length-at-birth estimated as mean of overlapping fetus and neonate TBL.
[c]Asymptotic length estimated from length frequency distribution.
[d]Asymptotic length estimated using a single Gompertz growth model.
[e]Asymptotic length estimated as mean TBL of individuals >25 years.
[f]Asymptotic length estimated using a single von Bertalanffy growth model.
[g]Asymptotic length estimated using a two-phase von Bertalanffy growth model.
[h]Age estimated using less reliable method: acid etching.
[i]Age estimated using less reliable method: transverse tooth sections.
Sources: 1, Martin et al. (1987); 2, Bloch et al. (1993a); 3, Lockyer (1993); 4, Sigurjonsson et al. (1993); 5, Sergeant (1962a); 6, Kasuya et al. (1988); 7, Crespo et al. (1985); 8, Soto et al. (2017); 9, this study.

Bloch et al. (1993a) off the Faroe Islands, and Sergeant (1962a) off Newfoundland, with both studies again estimating larger mean length-at-birth for the northern subspecies than those reported for the southern subspecies in this study (Newfoundland: 178 cm males [59 fetuses: 31 calves] and 174 cm females [49 fetuses: 43 calves]; Faroe Islands: 177 cm males and females combined [49 fetuses: 39 calves]; New Zealand: 171 cm males and females combined [7 fetuses: 15 calves]).

The overlap in lengths between the largest fetus (176 cm) and the smallest new-born calf (160 cm) in the current study is less than that found for *G. m. melas* off Newfoundland (190 and 165 cm; Sergeant 1962a) and the Faroe Islands (191 and 163 cm; Bloch 1993a). No fetuses measured over 176 cm in the New Zealand data, which in turn resulted in a lower estimated length-at-birth using both the logistic regression and the mean-overlap statistic. The smaller length-at-birth obtained may be due to undersampling of larger sized fetuses, although it seems unlikely near-term fetuses would be missed by chance given that the estimated peak calving period (i.e., early austral summer; Betty 2019) coincides with the peak stranding season (i.e., late austral spring through austral summer; Betty et al. 2020). The smaller estimated length-at-birth for *G. m. edwardii* therefore may represent true morphological variations between the northern and southern subspecies of LFPW.

The mean length of calves that do not possess a neonatal line in the tooth, or have a neonatal line forming (mean neonatal length), should not be considered an estimate of length-at-birth; it is unavoidably upwardly biased because only postnatal calves are considered. The fact that this method returned the highest estimates in this study (182 cm) and in the Faroe Islands study (200 cm) indicates that the neonatal line is not formed exactly at birth, but several weeks or perhaps months later, as previously suggested for the northern subspecies *G. m. melas* by Bloch et al. (1993a) and also for the Indo-Pacific bottlenose dolphin (*Tursiops aduncus*) by Kemper et al. (2019).

Growth.—Although the von Bertalanffy growth model was selected in this study due to slightly lower AIC scores for both males and females, the Gompertz growth model also adequately described growth in the species (and was the preferred growth model for *G. m. melas*; Bloch et al. 1993a). The von Bertalanffy growth model for female *G. m. edwardii* indicated an early period of rapid growth, followed by a decrease in growth velocity and a period of sustained but slower growth until attainment of asymptotic size (Fig. 6). In contrast, a secondary growth spurt around the average age at attainment of sexual maturity was apparent for males, which was followed by a period of slower growth, although the growth model did not reach a clear asymptote (see Figs. 5, 6). A review of published

data on geographical variations in the predicted asymptotic TBL value, estimated age at attainment of asymptotic length, and maximum TBLs recorded for LFPWs is listed in Table 5. Estimates of asymptotic and maximum lengths of LFPWs in the current study are similar to those previously reported for both *G. m. edwardii* and *G. m. melas* elsewhere, with the exception of a longer estimated asymptotic length for female *G. m. melas* off Newfoundland (which was not estimated using a comparable modeling approach) and a much longer maximum female body length recorded for LFPWs off the British coast (see Table 5).

LFPWs off New Zealand appear to continue to grow after attainment of sexual maturity (females ASM = 6.7 years, Betty 2019; males ASM = 13.5 years, Betty et al. 2019), albeit at a much-reduced rate, until well into old age (*ca.* 30 years for females and ≥ 40 years for males). The lack of a clear plateau in the male growth model may be an artifact of the small number of males older than 20 years of age (*n* = 12). However, other studies on the northern subspecies also have indicated a protracted growth pattern, particularly in males (Bloch et al. 1993a; Sigurjonsson et al. 1993). Physical maturity in *G. m. melas* off the Faroe Islands, determined from vertebral epiphyseal fusion, was reported to be reached at around 25 to 30 years of age for males and *ca.* 30 years for females (Bloch et al. 1993a). Growth curves for this region suggest that growth rates decline for both sexes at around 25 to 30 years and lengths of 570 and 450 cm for males and females, respectively (Bloch et al. 1993a). However, while some *G. m. melas* were found to attain physically maturity (vertebral fusion) around this age, others were still growing, resulting in the apparent protracted growth pattern (Bloch et al. 1993a) also observed in *G. m. edwardii* (particularly pronounced for males).

The existence of a secondary growth spurt in males has been reported in other delphinid species, including the common bottlenose dolphin (*Tursiops truncatus*; Cheal and Gales 1992) and Guiana dolphin (*Sotalia guianensis*; Rosas et al. 2003) and was suggested previously for *G. m. melas* by Kasuya et al. (1988). Sexual variation in asymptotic size and an extended period of male growth in the current study, may be a result of several factors, including sexual variation in foraging ecology (Cockcroft and Ross 1990) due to resource partitioning (Bernard and Hohn 1989), as well as differing reproductive strategies among the sexes (Read et al. 1993). Female LFPWs attain sexual maturity much earlier than males (Desportes et al. 1993; Martin and Rothery 1993; Betty 2019) and at that time, females divert available energy from growing in size to reproduction (i.e., gestation and lactation; Reynolds et al. 2000). In contrast, male growth velocity spikes around the age of sexual maturation, and growth continues to surpass that of females after attainment of sexual maturity, suggesting that male size may be an important factor in the mating system of LFPWs. If male reproductive success is correlated with size, as observed in many other sexually dimorphic mammals (Clutton-Brock 1988), the continued male growth after attainment of sexual maturity may suggest investment in future reproduction through either contest competition or female choice (Read et al. 1993). Although the costs

of this continued period of growth are not well understood, in other sexually dimorphic mammals, prolonged or accelerated growth is associated with higher rates of natural mortality in males (Case 1978; Read et al. 1993). This also may be the case in LFPWs, where the mortality rate of males is considerably higher than females (Bloch et al. 1993a; Betty et al. 2019; Betty et al. 2020).

The results of the growth models employed in this study are important for two reasons. First, they document detailed growth curves for *G. m. edwardii* in New Zealand waters for the first time; information that can be used to differentiate management units in the southern subspecies, when more data become available. For example, models of body growth were employed to differentiate or confirm management units for harbor porpoises (*Phocoena phocoena*) in the Northeast Atlantic (Murphy et al. 2020). Second, estimates of life history parameters presented herein can be used as a baseline in future assessments of population condition in the region. In other marine mammal populations, temporal increases observed in body growth rates have been attributed to greater prey availability *per capita* associated with declines in population sizes (Lockyer 1978, 1981; Hanks 1981; Kasuya 1991; Trites and Bigg 1992). In contrast, a decline in body growth rates over time may reflect a poor body condition of individuals in population due to limited available resources (Hanks 1981).

Allometry and sexual dimorphism.—Sexual size dimorphism was evident in the current study, with male *G. m. edwardii* being significantly larger than females in TBL, and in 12 of the additional 13 measurements taken. Genital slit length was the only measurement for which female *G. m. edwardii* exhibited a higher growth rate than males. However, this measurement is not comparable between the sexes due to the sexual variation in the position of the genitals. Mean TBLs obtained for physically mature (i.e., TBL above 0.9 × estimated asymptotic length) males and females were 550 and 432 cm, respectively, resulting in an SSD ratio of 1.27. A comparable SSD ratio of 1.34 was calculated for the northern subspecies of LFPW by Dines et al. (2015) using previously published data. The degree of SSD within LFPWs could be related to several biological factors, including behavior, social structure, mating system, the sex ratio of the breeding population, and/or environmental factors, such as habitat, distribution, diet, and prey abundance, as suggested for other odontocete species (Murphy and Rogan 2006). The extent of SSD varies widely among the odontocetes, with some of the most pronounced SSD ratios found in the sperm whale (1.64), SFPW (1.41), northern LFPW (1.34), northern right whale dolphin (*Lissodelphis borealis*; 1.34), narwhal (*Monodon monoceros*; 1.23), and killer whale (1.19) (reviewed by Dines et al. 2015).

Evidence of sexual shape dimorphism also was observed in *G. m. edwardii*, with mature males having proportionally longer pectoral fins, taller dorsal fins, and wider tail flukes (in order of decreasing level of significance) than mature females of similar body lengths. Mature males also exhibited higher growth rates than mature females in all appendage measurements (i.e., pectoral fin length and width, fluke width and dorsal fin height).

Among other odontocetes, there is considerable diversity in sexual dimorphism, such as differences in the size and shape of appendages, and other external structures, including the existence of postanal humps in mature males (Ngqulana et al. 2017, Mesnick and Ralls 2018). Longer and broader tail flukes and pectoral fins that have been reported in some odontocete males may function to give better propulsion (Mesnick and Ralls 2018) and to maintain hydrodynamic stability (Clark and Odell 1999). Dorsal fins of adult males are particularly exaggerated and erect in some species, e.g., killer whales (Clark and Odell 1999), the significance of which is not well understood, but they may serve a thermoregulatory function and/or a visual signal in mating interactions (Mesnick and Ralls 2018). Given that there is no evidence for male combat in killer whales or pilot whales, Dines et al. (2015) noted that "their dimorphic characters appear to function as ornaments, rather than armaments". Interestingly, among the different forms both of killer whales and SFPWs, there are differences in the relative degree of both sexual size and shape dimorphism of the dorsal fin (Durban et al. 2017, Kasuya 2017). Similar differences appear to occur between the two LFPW subspecies; sexual shape dimorphism in pectoral fins and tail flukes is evident in both subspecies (Bloch et al. 1993b), although only males of the southern subspecies *G. m. edwardii* exhibit a larger dorsal fin height relative to body size. Such differences are likely due to variation in ecology and sociality among subspecies or populations (Mesnick and Ralls 2018), although this has not been tested.

The current study presents detailed descriptions of growth, allometry, and sexual dimorphism of the southern LFPW subspecies, *G. m. edwardii*, using data collected from MSEs on the New Zealand coast. Age-related changes in growth rates between male and female LFPWs and strong evidence of sexual size dimorphism are demonstrated, with males attaining a larger body size than females (27% larger on average). Male LFPWs attained a greater asymptotic size than females due to a secondary growth spurt and a more prolonged period of growth. Sexual shape dimorphism also was evident in appendage measurements, with mature males having proportionally longer pectoral fins, taller dorsal fins, and wider tail flukes than mature females. Some of these features may be selected for as precopulatory traits and/or enabling maneuverability for a larger body size in males.

This study provides new insights into the life history of LFPWs in a region where empirical data have been scarce. Comparisons with northern hemisphere data show contrasts that increase our understanding of the species. For example, estimated length-at-birth and maximum ages for the southern LFPW subspecies are lower than previously reported for the northern LFPW subspecies. These differences, when combined with other information on their life history, may indicate subspecies or population-level differences in morphology, longevity, and sociality. Our research also provides guidance on how data collected from MSEs can be used to better understand age, growth, and morphology of cetaceans. As a consequence, this study can be used to inform future research which can further add to the growing body of knowledge on pelagic delphinids.

CONFLICT OF INTEREST

None declared.

SUPPLEMENTARY DATA

Supplementary data are available at *Journal of Mammalogy* online.

Supplementary Data SD1.—Code for the Bayesian logistic regression model used to estimate median length-at-birth for long-finned pilot whales (*Globicephala melas edwardii*) stranded on the New Zealand coast. The model was fitted using Stan (Stan Development Team 2021) in R (R Development Core Team 2021).

Supplementary Data SD2.—Prior predictive simulation of P (probability of birth) given x (length) for long-finned pilot whales (*Globicephala melas edwardii*) stranded on the New Zealand coast based on prior distributions for Bayesian logistic regression model parameters $m = l_{50} \sim N(171, 20)$ and $w = \omega \sim N^+(0, 1)$. The simulation was fitted using Stan (Stan Development Team 2021) in R (R Development Core Team 2021).

Supplementary Data SD3.—Posterior distribution of the difference in estimated median length-at-birth (with point mean, and 66% and 95% highest posterior density intervals) between male and female long-finned pilot whales (*Globicephala melas edwardii*) stranded on the New Zealand coast (*n* = 169).

Supplementary Data SD4.—Sex vs. seven linear body measurements of long-finned pilot whales (*Globicephala melas edwardii*) stranded on the New Zealand coast (1948–2017). Total length (male: *n* = 188, female *n* = 519); Ujaw anus (male: *n* = 43, female *n* = 119); Ujaw genital (male: *n* = 64, female *n* = 186); Ujaw dorsal (male: *n* = 71, female *n* = 184); Ujaw pectoral (male: *n* = 80, female *n* = 216); Ujaw blowhole (male: *n* = 68, female *n* = 176); and Ujaw gape (male: *n* = 48, female *n* = 113). Colors represent the individuals' sex: female = red, male = blue. Cor = Spearman's rank correlation coefficients. All measurements in cm.

Supplementary Data SD5.—Sex vs. total body length, four appendage measurements, axillary girth, snout and genital slit length of long-finned pilot whales (*Globicephala melas edwardii*) stranded on the New Zealand coast (1948–2017). Total length (male: *n* = 188, female *n* = 519); height dorsal (male: *n* = 31, female *n* = 91); pectoral length (male: *n* = 67, female *n* = 183); pectoral width (male: *n* = 38, female *n* = 87); fluke width (male: *n* = 53, female *n* = 139); Axill girth (male: *n* = 44, female *n* = 125); Snout length (male: *n* = 26, female *n* = 80); and Genital slit (male: *n* = 14, female *n* = 37). Colors represent the individuals' sex: female = red, male = blue. Cor = Spearman's rank correlation coefficients. All measurements in cm.

LITERATURE CITED

Agbayani S., Fortune S.M.E., Trites A.W. 2020. Growth and development of North Pacific gray whales (*Eschrichtius robustus*). Journal of Mammalogy 101:742–754.

Augusto J.F., Frasier T.R., Whitehead H. 2013. Using photography to determine sex in pilot whales (*Globicephala melas*) is not possible: males and females have similar dorsal fins. Marine Mammal Science 29:213–220.

Berkenbusch K.E., Abraham R., Torres L.G. 2013. New Zealand marine mammals and commercial fisheries. New Zealand Aquatic Environmental and Biodiversity Report No. 119. Ministry for Primary Industries. Wellington, New Zealand.

Bernard H.J., Hohn A.A. 1989. Differences in feeding habits between pregnant and lactating spotted dolphins (*Stenella attenuata*). Journal of Mammalogy 70:211–215.

Best P.B. 1970. The sperm whale (*Physeter catadon*) off the west coast of South Africa. 5. Age, growth and mortality. Division of Sea Fisheries Investigational Report 79:1–27.

Betty E.L. 2019. Life history of the long-finned pilot whale (*Globicephala melas edwardii*); insights from strandings on the New Zealand coast [dissertation]. Auckland University of Technology, Auckland, New Zealand.

Betty E.L., Bollard B., Murphy S., Ogle M., Hendriks, H., Orams M.B., Stockin K.A. 2020. Using emerging hot spot analysis of stranding records to inform conservation management of a data-poor cetacean species. Biodiversity and Conservation 29:643–665.

Betty E.L., Stockin K.A., Smith A.N.H., Bollard B., Orams M.B., Murphy S. 2019. Sexual maturation in male long-finned pilot whales (*Globicephala melas edwardii*): defining indicators of sexual maturity. Journal of Mammalogy 100:1387–1402.

Bloch D., Lockyer C., Zachariassen M. 1993a. Age and growth parameters of the long-finned pilot whale off the Faroe Islands. Reports of International Whaling Commission 14:163–208.

Bloch D., Zachariassen M., Zachariassen P. 1993b. Some external characters of the long-finned pilot whale off the Faroe Islands and a comparison with the short-finned pilot whale. Reports of the International Whaling Commission 14:118–135.

Börjesson P., Read A.J. 2003. Variation in timing of conception between populations of the harbor porpoise. Journal of Mammalogy 84:948–955.

Brabyn M.W. 1991. An analysis of the New Zealand whale stranding record. Science and Research Series No. 29. New Zealand Department of Conservation, Wellington, New Zealand.

Case T.J. 1978. On the evolution and adaptive significance of postnatal growth rates in the terrestrial vertebrates. The Quarterly Review of Biology 53:243–282.

Caughley G. 1977. Analysis of vertebrate populations. Wiley.

Cheal A., Gales N. 1992. Growth, sexual maturity and food intake of Australian Indian Ocean bottlenose dolphins, *Tursiops truncatus*, in captivity. Australian Journal of Zoology 40:215–223.

Clark S.T., Odell D.K. 1999. Allometric relationships and sexual dimorphism in captive killer whales (*Orcinus orca*). Journal of Mammalogy 80:777–785.

Clutton-Brock T.H. 1988. Reproductive success: studies of individual variation in contrasting breeding systems. University of Chicago Press, Chicago, USA.

Cockcroft V., Ross G. 1990. Age, growth and reproduction of bottlenose dolphins *Tursiops truncatus* from the east coast of southern Africa. Fishery Bulletin 88:289–302.

Crespo E., Pagnoni G., Pedraza S. 1985. Structure of a long-finned pilot whale school stranded in Patagonia. Scientific Reports of the Whales Research Institute 36:97–106.

Danil K., Chivers S.J. 2007. Growth and reproduction of female short-beaked common dolphins, *Delphinus delphis*, in the eastern tropical Pacific. Canadian Journal of Zoology 85:108–121.

Denuncio P., Negri M.F., Bastida R., Rodríguez D. 2018. Age and growth of Franciscana dolphins from northern Argentina. Journal of the Marine Biological Association of the United Kingdom 98:1197–1203.

Desportes G., Andersen L., Bloch D. 1994. Variation in foetal and postnatal sex ratios in long-finned pilot whales. Ophelia 39:183–196.

Desportes G., Saboureau M., Lacroix A. 1993. Reproductive maturity and seasonality of male long-finned pilot whales, off the Faroe Islands. Reports of the International Whaling Commission 14:233–262.

Dines J.P., Mesnick S.L., Ralls K., May-Collado L., Agnarsson I., Dean M.D. 2015. A trade-off between precopulatory and postcopulatory trait investment in male cetaceans. Evolution; International Journal of Organic Evolution 69:1560–1572.

Donovan G., Lockyer C., Martin A., editors. 1993. Biology of Northern Hemisphere pilot whales. Reports of the International Whaling Commission. 14. Cambridge, UK.

Durban J.W., Fearnbach H., Burrows D.G., Ylitalo G.M., Pitman R.L. 2017. Morphological and ecological evidence for two sympatric forms of Type B killer whale around the Antarctic Peninsula. Polar Biology 40:231–236.

Evans K., Hindell M.A. 2004. The age structure and growth of female sperm whales (*Physeter macrocephalus*) in southern Australian waters. Journal of Zoology 263:237–250.

Fitzhugh H.A., Jr. 1976. Analysis of growth curves and strategies for altering their shape. Journal of Animal Science 42:1036–1051.

Hanks J. 1981. Characterisation of population condition. In: Fowler C.W., Smith A.T., editors. Dynamics of large mammal populations. Wiley; p. 47–73.

Hohn A.A., Fernandez S. 1999. Biases in dolphin age structure due to age estimation technique. Marine Mammal Science 15:1124–1132.

Huisman J., Olff H., Fresco L.F.M. 1993. A hierarchical set of models for species response analysis. Journal of Vegetation Science 4:37–46.

Isaac J.L. 2005. Potential causes and life-history consequences of sexual size dimorphism in mammals. Mammal Review 35:101–115.

Jefferson T.A., Hung S.K., Robertson K.M., Archer F.I. 2012. Life history of the Indo-Pacific humpback dolphin in the Pearl River Estuary, southern China. Marine Mammal Science 28:84–104.

Kasuya T. 1991. Density dependent growth in North Pacific sperm whales. Marine Mammal Science 7:230–257.

Kasuya T. 2017. Small cetaceans of Japan: exploitation and biology. CRC Press, Taylor & Francis Group, Boca Raton, Florida, U.S.A.

Kasuya T., Marsh H. 1984. Life history and reproductive biology of the short-finned pilot whale, *Globicephala macrorhynchus*, off the Pacific Coast of Japan. Reports of the International Whaling Commission 6:259–310.

Kasuya T., Matsui S. 1984. Age determination and growth of the short-finned pilot whale off the Pacific Coast of Japan. The Scientific Reports of the Whales Research Institute 35:57–91.

Kasuya T., Sergeant D.E., Tanaka K. 1988. Re-examination of life history parameters of long-finned pilot whales in the Newfoundland waters. Scientific Reports of the Whales Research Institute 39:103–119.

Kasuya T., Tai S. 1993. Life history of short-finned pilot whale stocks off Japan and a description of the fishery. Reports of the International Whaling Commission 14:439–473.

Kay M. 2021. tidybayes: tidy data and Geoms for Bayesian models. doi: 10.5281/zenodo.5138624, R package version 3.0.0. http://mjskay.github.io/tidybayes/.

Kemper C.M., Milano S., Ciraolo A.C. 2019. Neonatal line may develop after birth in the Indo-Pacific bottlenose dolphin (*Tursiops aduncus*). Canadian Journal of Zoology 97:685–695.

Laird A.K. 1966. Postnatal growth of birds and mammals. Growth 30:349–363.

Laws R.M. 1959. The foetal growth rates of whales with special reference to the fin whale, *Balaenoptera physalus* Linn. Discovery Reports 29:281–308.

Lockyer C. 1978. A theoretical approach to the balance between growth and food consumption in fin and sei whales, with special reference to the female reproductive cycle. Report of International Whaling Commission 28:243–249.

Lockyer C. 1981. Estimates of growth and energy budget for the sperm whale, *Physeter catadon*. In: FAO Advisory Committee on Marine Resources. Working Party on Marine Mammals. FAO, La Jolla, California; p. 489–504.

Lockyer C. 1993. A report on patterns of deposition of dentine and cement in teeth of pilot whales, genus *Globicephala*. Reports of the International Whaling Commission 14:137–161.

Lockyer C., Desportes G., Waters T. 1987. Preliminary studies of pilot whales from Faroese waters since 1986: age determination. Paper SC/39/SM16 presented to the IWC Scientific Committee.

Martin A.R., Reynolds P., Richardson M.G. 1987. Aspects of the biology of pilot whales (*Globicephala melaena*) in recent mass strandings on the British coast. Journal of Zoology 211:11–23.

Martin A.R., Rothery P. 1993. Reproductive parameters of female long-finned pilot whales (*Globicephala melas*) around the Faroe Islands. Reports of the International Whaling Commission 14:263–304.

Mattson M.C., Mullin K.D., Ingram G.W., Hoggard W. 2006. Age structure and growth of the bottlenose dolphin (*Tursiops truncatus*) from strandings in the Mississippi Sound region of the north-central Gulf of Mexico from 1986 to 2003. Marine Mammal Science 22:654–666.

McFee W.E., Schwacke J.H., Stolen M.K., Mullin K.D., Schwacke L.H. 2010. Investigation of growth phases for bottlenose dolphins using a Bayesian modeling approach. Marine Mammal Science 26:67–85.

Mesnick S., Ralls K. 2018. Sexual dimorphism. In: Würsig B., Thewissen J.G M., Kovacs K.M., editors. Encyclopedia of marine mammals. Third Edition. Academic Press; p. 848–853.

Moore J.E., Read A.J. 2008. A Bayesian uncertainty analysis of cetacean demography and bycatch mortality using age-at-death data. Ecological Applications: A Publication of the Ecological Society of America 18:1914–1931.

Murphy S., Petitguyot M.A.C, Jepson P.D., Deaville R., Lockyer C., Barnett J., Perkins M., Penrose R., Davison N.J., Minto C. 2020. Spatio-temporal variability of harbor porpoise life history parameters in the North-East Atlantic. Frontiers in Marine Science. 7:502352.

Murphy S., Rogan E. 2006. External morphology of the short-beaked common dolphin, *Delphinus delphis*: growth, allometric relationships and sexual dimorphism. Acta Zoologica 87:315–329.

Murphy S., Winship A., Dabin W., Jepson P., Deaville R., Reid R., Spurrier C., Rogan E., Lopez A., Gonzalez A., et al. 2009. Importance of biological parameters in assessing the status of *Delphinus delphis*. Marine Ecology Progress Series 388:273–291.

Ngqulana S.G., Hofmeyr G.J.G., Plön S. 2017. Sexual dimorphism in long-beaked common dolphins (*Delphinus capensis*) from KwaZulu-Natal, South Africa. Journal of Mammalogy 98:1389–1399.

Norris K.S. 1961. Standardized methods for measuring and recording data on the smaller cetaceans. Journal of Mammalogy 42:471–476.

Perrin W., Coe J., Zweifel J. 1976. Growth and reproduction of the spotted porpoise, *Stenella attenuata*, in the offshore eastern tropical Pacific. Fishery Bulletin 74:229–268.

Perrin W.F., Myrick A.C.J. 1980. Report of the Workshop. Age determination of toothed whales and sirenians. Reports of the International Whaling Commission 3:1–50.

Plön S., Heyns-Veale E.R., Smale M.J., Froneman P.W. 2020. Life history parameters and diet of Risso's dolphins, *Grampus griseus*, from southeastern South Africa. Marine Mammal Science 36:786–801.

R Development Core Team. 2021. R: a language and environment for statistical computing. Foundation for Statistical Computing, R., Vienna, Austria. www.R-project.org/.

Read A.J., Tolley K.A. 1997. Postnatal growth and allometry of harbour porpoises from the Bay of Fundy. Canadian Journal of Zoology 75:122–130.

Read A.J., Wells R.S., Hohn A.A., Scott M.D. 1993. Patterns of growth in wild bottlenose dolphins, *Tursiops truncatus*. Journal of Zoology 231:107–123.

Reynolds J.E., Wells R.S., Eide S.D. 2000. The bottlenose dolphin: biology and conservation. University Press of Florida, Gainesville, Florida.

Rosas F., Barreto A., Monteiro-Filho E. 2003. Age and growth of the estuarine dolphin (*Sotalia guianensis*) (Cetacea, Delphinidae) on the Parana Coast, southern Brazil. Fishery Bulletin 101:377–383.

Salas-Eljatib C., Fuentes-Ramirez A., Gregoire T.G., Altamirano A., Yaitul V. 2018. A study on the effects of unbalanced data when fitting logistic regression models in ecology. Ecological Indicators 85:502–508.

Schmidt-Nielsen K. 1993. Scaling: why is animal size so important? Cambridge University Press, Cambridge, UK.

Schroder C., Castle P. 1998. Life history parameters and polychlorinated biphenyls (PCBs) in long-finned pilot whales (*Globicephala melas*) from New Zealand strandings. A report to WWF - New Zealand. Wellington, New Zealand.

Sergeant D.E. 1962a. The biology of the pilot or pothead whale *Globicephala meleana* (Traill) in Newfoundland waters. Bulletin of the Fisheries Research Board of Canada 132:1–84.

Sergeant D.E. 1962b. On the external characters of the blackfish or pilot whale genus *Globicephala*. Journal of Mammalogy 43:395–413.

Shine R. 1989. Ecological causes for the evolution of sexual dimorphism: a review of the evidence. The Quarterly Review of Biology 64:419–461.

Sigurjonsson J., Vikingsson G., Lockyer C. 1993. Two mass strandings of pilot whales *Globicephala melas* on the coast of Iceland. Reports of the International Whaling Commission 14:407–423.

Soto F.A., Grandi M.F., Garcia N.A., Crespo E.A., Dans S.L. 2017. Reproductive parameters of female long-finned pilot whales (*Globicephala melas edwardii*) from the Southwestern Atlantic. Zoological Studies 56:1–12.

Stan Development Team. 2021. Stan modeling language users guide and reference manual, 2.27. https://mc-stan.org

Stolen M.K., Odell D.K., Barros N.B. 2002. Growth of bottlenose dolphins (*Tursiops truncatus*) from the Indian River lagoon system, Florida, U.S.A. Marine Mammal Science 18:348–357.

Trites A.W., Bigg M. 1992. Changes in body growth of northern fur seals from 1958 to 1974: density effects or changes in the ecosystem? Fisheries Oceanography 1:127–136.

Vehtari A., Gabry J., Magnusson M., Yao Y., Bürkner P., Paananen T., Gelman A. 2020. loo: efficient leave-one-out cross-validation and WAIC for Bayesian models. R package version 2.4.1. https://mc-stan.org/loo/

Vehtari A., Gelman A., Gabry J. 2017. Practical Bayesian model evaluation using leave-one-out cross-validation and WAIC. Statistics and Computing 27:1413–1432.

von Bertalanffy L. 1938. A quantitative theory of organic growth (inquiries on growth laws. II). Human Biology 10:181–213.